

Boson features in STM spectra of cuprate superconductors: Weak-coupling phenomenology

Sumiran Pujari and C. L. Henley

Department of Physics, Cornell University, Ithaca, New York 14853-2501

We derive the shape of the high-energy features due to a weakly coupled boson in cuprate superconductors, as seen experimentally in $\text{Bi}_2\text{Sr}_2\text{Ca}_1\text{Cu}_2\text{O}_{8+x}$ (BSCCO) by Lee *et al* [Nature 442, 546 (2006)]. A simplified model is used of d -wave Bogoliubov quasiparticles coupled to Einstein oscillators with a momentum independent electron-boson coupling and an approximate analytic fitting form is derived, which allows us (a) to extract the boson mode's frequency, and b) to estimate the electron-boson coupling strength.

PACS numbers: 74.55.+v, 72.10.Fk, 73.20.At, 74.72.ah

Scanning tunneling microscopy (STM), applied to the superconducting cuprate $\text{Bi}_2\text{Sr}_2\text{Ca}_1\text{Cu}_2\text{O}_{8+x}$ (BSCCO 2212) [1], found a feature in the density of states (DOS) at an energy well above the energy scale of the so-called coherence peak energy (Fig. 1), and attributed it to an electron-boson coupling. In conventional (s-wave) superconductors (e.g. Hg, Pb, Al), such features due to electron-phonon coupling were known in tunneling spectra from superconductor-insulator-normal metal junctions [2, 3]. The phonon frequencies inferred from the tunneling feature agreed with the phonon density of states inferred from neutron scattering; furthermore, the phonon-mediated superconducting T_c and gap were correctly predicted [2] from the tunneling using the Eliashberg formalism [4]. In the case of cuprates, the mechanism for superconductivity is not established, and there are divergent opinions whether the mode observed by Lee *et al* contributes to the pairing [1, 7–9].

In BSCCO, the pairing strength is highly inhomogeneous at the nanoscale [11, 12], as inferred from the spatial fluctuations of the energy E_{coh} of the “coherence peak” in STM spectra (Figure 1). Lee *et al* discovered that the boson feature's energy E_{bos} “floats” with the same inhomogeneity as E_{coh} , namely $E_{\text{bos}} = E_{\text{coh}} + \hbar\Omega_0$ with a (spatially uniform) boson

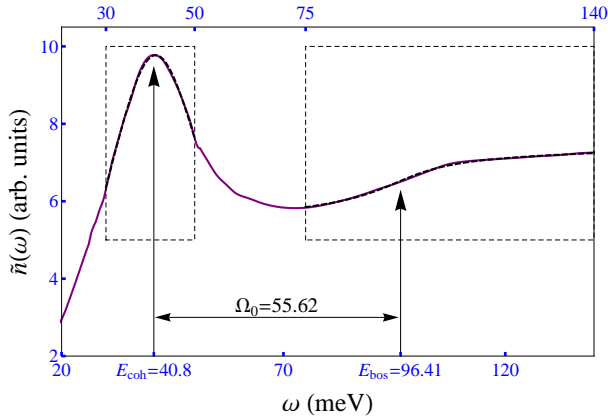


FIG. 1: [COLOR ONLINE] A typical measured STM spectrum in BSCCO (proportional to DOS $n(\omega)$) as a function of energy E ; the data was provided by Jacob Alldredge. Energies of the “coherence peak” E_{coh} and boson feature E_{bos} are indicated. Boxes show energy windows used to fit the analytic form (see Fig. 3, below.)

frequency Ω_0 . To infer E_{bos} , they identified it as the inflection point in $n(\omega)$ before the feature. In this paper, we improve on this recipe by deriving an analytic formula for the boson feature, starting from the simplest phenomenological model of a cuprate and using basic RPA calculations. *Our focus here is the energy dependence rather than the spatial modulations [13, 14] of this feature.* One prior calculation [5] addressed the same question of extracting Ω_0 from the shape of the DOS of BSCCO, using more elaborate (Eliashberg) calculation, but in an entirely numerical framework, making the interpretation harder and the method impractical for extensive fitting.

We first ask just what point in the feature is to be identified as E_{bos} : our recipe implies a value for $\hbar\Omega$ in agreement with the analysis in Ref. [1]. Secondly, we ask how can one extract the electron-boson coupling strength; our results indicate it is indeed small enough that our weak-coupling approximation is justified, and furthermore this coupling alone is unlikely to explain the magnitude of the superconducting gap.

Weak-coupling Model —

We begin by setting up the simplest possible model, taking the electron-boson coupling as a small perturbation to an already superconducting fermion dispersion of the standard mean-field form (as in Ref. 13), and then setting up the DOS calculation within the RPA approximation. Our analysis is agnostic as to the boson's nature, which is sometimes argued to be magnetic [9], but usually considered to be an oxygen vibration, on account of the O^{18} isotope effect [1].

Our bare fermion Hamiltonian has the usual mean-field form

$$\mathcal{H} = \sum_{\mathbf{k}, \sigma} \epsilon(\mathbf{k}) c_{\mathbf{k}, \sigma}^\dagger c_{\mathbf{k}, \sigma} + \Delta(\mathbf{k}) c_{\mathbf{k}, \sigma} c_{-\mathbf{k}, -\sigma} + h.c. \quad (1)$$

where $\epsilon(\mathbf{k})$ is the normal-state band dispersion, for which (in all numerical calculations in this paper) we adopt Norman's six-parameter tight-binding fit to ARPES data on BSCCO [10]. The quasiparticle dispersion is then $E(\mathbf{k}) = \sqrt{\epsilon(\mathbf{k})^2 + \Delta(\mathbf{k})^2}$, where we will assume d -wave pairing with

$$\Delta(\mathbf{k}) \equiv \frac{\Delta_0}{2} [\cos(k_x) - \cos(k_y)]. \quad (2)$$

We (plausibly) approximate the bosonic mode as a dispersionless (Einstein) oscillator at frequency Ω_0 , and assume an

electron-phonon coupling

$$\mathcal{H}_{e\text{-ph}} = \frac{1}{\sqrt{N}} \sum_{\mathbf{k}, \mathbf{q}, \sigma} g(\mathbf{q}) c_{\mathbf{k}+\mathbf{q}, \sigma}^\dagger c_{\mathbf{k}, \sigma} (b_{-\mathbf{q}} + b_{\mathbf{q}}^\dagger) \quad (3)$$

where $b_{\mathbf{q}}^\dagger$ and $b_{\mathbf{q}}$ are the bosonic creation and annihilation operators, and N is the number of lattice sites. For simplicity we work through the case $g(\mathbf{q}) \equiv g$; after completing that, we will revisit the more general case with a momentum-dependent $g(\mathbf{q})$.

Our object, the DOS, is defined as the trace of the electron term in the Green's function:

$$n(\omega) \equiv -\frac{1}{\pi} \text{Tr}_{\mathbf{k}} \text{Im} G_{11}(\mathbf{k}, \omega), \quad (4)$$

where $\text{Tr}_{\mathbf{k}} \equiv a^2 \int_{\text{B.Z.}} d^2\mathbf{k}/(2\pi)^2$, and the integral is over the Brillouin zone. In the 2×2 Nambu formalism, the *bare* Green's function is given by

$$\underline{G}^0(\mathbf{k}; \omega)^{-1} = \begin{pmatrix} \omega - \epsilon(\mathbf{k}) & \Delta(\mathbf{k}) \\ \Delta(\mathbf{k})^* & \omega + \epsilon(\mathbf{k}) \end{pmatrix}. \quad (5)$$

We shall henceforth use Pauli matrices $\underline{\tau}_i$, and adopt the gauge in which Δ_0 is real: thus $\underline{G}^0 = [E\underline{1} + \epsilon(\mathbf{k})\underline{\tau}_3 + \Delta(\mathbf{k})\underline{\tau}_1]/[\omega^2 - E(\mathbf{k})^2]$. The boson propagator has the form

$$D(\mathbf{q}; \Omega) = \frac{1}{2} \left(\frac{1}{\Omega - \Omega_0} - \frac{1}{\Omega + \Omega_0} \right) \equiv D(\Omega). \quad (6)$$

Self-Energy and density of states due to the boson —

The boson feature enters the DOS via the dressed Green's function, in the RPA approximation,

$$\underline{G}(\mathbf{k}, \omega)^{-1} = \underline{G}^0(\mathbf{k}, \omega)^{-1} - \underline{\Sigma}(\mathbf{k}, \omega). \quad (7)$$

Because Ω_0 and $D(\Omega)$ were momentum-independent, so is the electronic self energy, reducing (at lowest order in g) to $\underline{\Sigma}(\mathbf{k}, \omega) \equiv \underline{\Sigma}(\omega)$, where

$$\underline{\Sigma}(\omega) = g^2 \int \frac{d\Omega}{2\pi} D(\Omega) \text{Tr}_{\mathbf{q}} \{ \underline{\tau}_3 \underline{G}^0(\mathbf{k} - \mathbf{q}; \omega - \Omega) \underline{\tau}_3 \} \quad (8)$$

After a contour evaluation of the Ω integral Eq. (8) reduces to

$$\underline{\Sigma}(\omega) = \frac{g^2}{2} \text{Tr}_{\mathbf{k}} \left\{ \frac{(\omega + \Omega_0)\underline{1} + \epsilon(\mathbf{k})\underline{\tau}_3 - \Delta(\mathbf{k})\underline{\tau}_1}{(\omega + \Omega_0)^2 - E(\mathbf{k})^2} + \frac{\Omega_0(\underline{1} + \frac{\epsilon(\mathbf{k})}{E(\mathbf{k})}\underline{\tau}_3 - \frac{\Delta(\mathbf{k})}{E(\mathbf{k})}\underline{\tau}_1)}{[\omega - E(\mathbf{k})]^2 - \Omega_0^2} \right\} \quad (9)$$

The off-diagonal ($\underline{\tau}_1$) terms in Eq. (9) vanish, $\Sigma_{12} = \Sigma_{21} \equiv 0$, since $\Delta_{\mathbf{k}}$ has d -wave symmetry (reverses sign under 90° rotations).

We write $n(\omega) = n_0(\omega) + \delta n(\omega)$, where $n_0(\omega)$ is the basic DOS in the absence of the phonon coupling [derived from (5)] and has the well-known ‘‘coherence peaks’’ centered at energy values $\pm E_{\text{coh}}$ close to $\pm \Delta_0$; $\delta n(\omega)$ contains contributions of

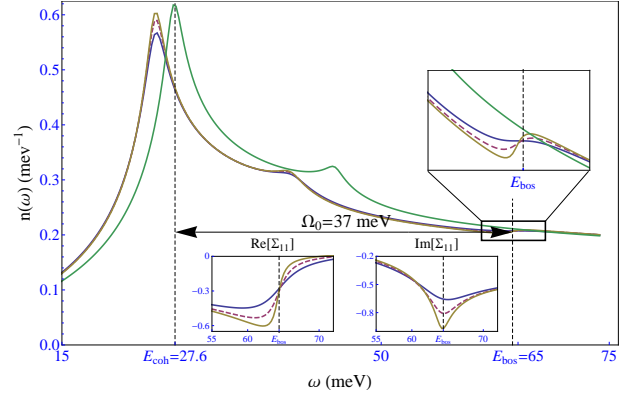


FIG. 2: [COLOR ONLINE] Numerically computed DOS as a function of energy. The standard six-parameter dispersion for BSCCO was used [10]; we chose the pairing amplitude to be $\Delta_0 = 0.2|t_1| \approx 29.6$ meV and the boson energy to be $\hbar\Omega_0 = 0.25|t_1| \approx 37$ meV, where t_1 is the nearest-neighbor hopping. Three different choices of damping are shown: from sharpest to flattest, $\eta = 0.005, 0.01$ and 0.02 (in units of t_1). Lower inset shows real and imaginary parts of the electron self-energy function. This has singularities at E_{bos} rounded by the damping.

order g^2 , in particular the boson feature. Writing the Taylor expansion of (7), we extract the terms in G_{11} linear in $\underline{\Sigma}$ and thus

$$\begin{aligned} \delta n(\omega) &= -\frac{1}{\pi} \text{Im} \text{Tr}_{\mathbf{k}} \left\{ \frac{[\omega + \epsilon(\mathbf{k})]^2 \Sigma_{11}(\omega) + |\Delta(\mathbf{k})|^2 \Sigma_{22}(\omega)}{[\omega^2 - E(\mathbf{k})^2]^2} \right\} \\ &\equiv \frac{1}{\pi} \text{Im} \{ I_1(\omega) \Sigma_{11}(\omega) + I_2(\omega) \Sigma_{22}(\omega) \}. \end{aligned} \quad (10)$$

This is the first version of our result, suitable for numerical fits [15], but requiring integrations over the zone at each iteration [for the key formulas (9) and (10). Note that in numerical calculations, we replace $\omega \rightarrow \omega + i\eta$ in (5), where $i\eta$ represents the physical quasiparticle damping (from all sources except our boson mode), a parameter found essential for fitting the ‘‘coherence peaks’’ in the DOS [16]. (It is easy to replace this energy-independent damping by $\eta(\omega)$, as used in Ref. [16].) Fig. 2 shows a representative numerical calculation of the self-energy function (inset) and the resulting DOS. We see a dip-hump shape, in agreement with experiment; E_{bos} falls between the dip and the hump similar to the assumption of Ref. [1].

Asymptotic Form near $E_{\text{bos}} = E_{\text{coh}} + \Omega_0$ —

We now extend our results to an approximate *analytic* formula, for the boson feature's shape, by treating not only the electron-phonon coupling g , but also the damping η as a small parameter: in the limit $\eta \rightarrow 0$ the feature is a singularity centered at $E_{\text{bos}} \equiv E_{\text{coh}} + \Omega_0$.

First recollect the origin of the familiar ‘‘coherence peak’’ in the basic DOS $n_0(\omega)$: it is a van Hove singularity due to the saddle points at $\mathbf{k} = (k_s, \pi)$ and equivalent momenta where the Fermi surface crosses the zone boundary. The pertinent pole in \underline{G}_0 is $\frac{1}{2}[\omega - E(\mathbf{k})]^{-1}\underline{1}$; there is no contribution from $\underline{\tau}_3$ due to the factor $\epsilon(\mathbf{k})$ which vanishes on the Fermi sur-

face. It is well known that $\text{Tr}_{\mathbf{k}}[\omega - E(\mathbf{k})]$ at a saddle gives a logarithmic singularity, so we find a singular part

$$n_0^{\text{sing}}(\omega) = -\frac{a^2 m^*}{\pi^2} \text{Re} f(\omega - E_{\text{coh}} + i\eta_{\text{coh}}) \quad (11)$$

with

$$f(z) \equiv \ln(m^* z / 4K_x K_y). \quad (12)$$

Here $E(\mathbf{k}) \approx E_{\text{coh}} + (k_x - k_s)^2 / 2m_x - (k_y - \pi/a)^2 / 2m_y$ near the saddle, $m^* \equiv \sqrt{m_x m_y}$, and K_x, K_y are cut-offs, representing the range of (k_x, k_y) within which this expansion is valid. For our parameters, $1/m^* = 94.07 \text{meV } a^2$, and we take $K_x = 0.5a^{-1}$ and $K_y = 0.06a^{-1}$ for later numerical calculations.

The self-energy $\underline{\Sigma}(E)$ has a singularity due to the same saddle point, with the pole of form $(\frac{1}{2})^2 g^2 \underline{\mathbb{I}}[\omega - E(\mathbf{k}) - \Omega_0]^{-1}$, coming from the second big term in (9). Clearly, integrating over \mathbf{k} gives the same logarithmic divergence, with its argument shifted by Ω_0 . Thus,

$$\underline{\Sigma}(\omega + i\eta) = \text{regular terms} + \frac{ig^2 a^2}{2\pi} m^* f(\omega - E_{\text{bos}} + i\eta) \underline{\mathbb{I}} \quad (13)$$

with $f(z)$ from (12). This behavior is confirmed by the inset of Fig. 2,

The $\underline{\mathbb{I}}$ dependence in (13) signifies that $\Sigma_{11} \approx \Sigma_{22}$ at the singularity. Thus (10) simplifies to

$$\delta n^{\text{sing}}(\omega) = \frac{1}{\pi} \text{Im}[\Sigma_{11}(\omega) I(E_{\text{bos}} + i\eta)], \quad (14)$$

with $I(\omega) \equiv [I_1(\omega) + I_2(\omega)]/2$ [see Eq. 10]

Thus our key asymptotic result is that $\delta n(\omega)$ has a *logarithmic* singularity at E_{bos} , rounded by the finite damping η . The result is a linear combination of a rounded step and a cut-off log divergence, with the exact shape (and the location of E_{bos} within it) depending on the phase angle in $I(\omega) \equiv |I(\omega)|e^{i\phi_I}$, which depends on the band structure [cf. Eq. (14)].

At $\omega = 115 \text{ meV}$, the rough dependence on damping is $I(\omega + i\eta) = 1.5 \times 10^{-5}(\eta - 15) + 0.7 \times 10^{-3}i$. Thus, the shape of $\delta n(\omega)$ is a (comparable) combination of a rounded *upwards* step from $\text{Re}\Sigma_{11}$ and a rounded logarithmic hump from $\text{Im}\Sigma_{11}$ leading to location of the boson mode frequency ω before the hump (as seen in numerics cf. Fig. 2).

We can attach physical interpretations to the real and imaginary parts of $\Sigma_{22}(\omega)$. The imaginary part represents an inelastic event in which a *real* phonon excitation is created; the real part represents the quasiparticle being dressed by *virtual* phonons.

Since the predicted feature includes a “step up”, we are in agreement with the recipe of Lee *et al* which placed E_{bos} at the inflection point *before the hump* of the boson feature, motivated by previous work on molecular vibrational features in electron tunneling [18, 19]. Refs. 5 and 6 located E_{bos} even lower, at the *minimum of the dip* in the dip-hump feature. As mentioned before, we also place E_{bos} *before* the hump but

Δ_0	44.23 meV	Ω_0	55.62 meV
β_{cal}	3.25×10^4	g	35.93 meV
η_{coh}	10.7 meV	η_{bos}	11.04 meV
a_{coh}	$3.08 \times 10^{-2} \text{ meV}^{-2}$	a_{bos}	$0.38 \times 10^{-2} \text{ meV}^{-2}$
b_{coh}	8.07 meV^{-1}	b_{bos}	6.93 meV^{-1}

TABLE I: Fit parameters for the “coherence peak” using Eq. (15) (left column) and for the boson feature using Eq. (16) (right column).

more specifically in between the hump and its preceding inflection point.

We can attempt to compare our self-energy functions with those of Ref. [5] [(Figure 3(c)], computed numerically from Eliashberg theory. $\text{Re}\Sigma_{ii}(\omega)$ is proportional to their $\text{Im}Z(\omega)$ which indeed resembles a (positive) log divergence, while $\text{Im}\Sigma_{ii} \propto 1 - Z(\omega)$ shows a rounded up step.

Fitting Scheme for the Experimental Boson Feature —

In this section, we translate our asymptotic forms to a simplified fitting scheme for our weak-coupling model and, by applying it to the experimental spectrum in Fig. 1, extract the E_{bos} and also obtaining the electron-phonon coupling g from the boson feature’s amplitude. [21] We consider the experimental signal to be in arbitrary units so we write it $\tilde{n}(\omega) = \beta_{\text{cal}} n(\omega)$, where the coefficient β_{cal} includes unknown factors such as the STM tip set-point. As the dispersion $\epsilon(\mathbf{k})$ is already known from ARPES [10], the “coherence peak” is sufficiently constrained that we can calibrate β_{cal} from it. We read off $E_{\text{coh}} = 40.8 \text{ meV}$ from the peak position in Fig. 1. From this, using $E_{\text{coh}} = E(\mathbf{k}_{\text{saddle}})$, we infer $\Delta_0 = 44.23 \text{ meV}$.

The saddle point of the quasiparticle dispersion at $\mathbf{k}_{\text{saddle}}$ contributes a logarithmic singularity to the DOS at the “coherence peak”:

$$n_0(\omega) = n^{\text{reg}}(\omega) + n_0^{\text{sing}}(\omega) \quad (15)$$

where $n_0^{\text{sing}}(\omega)$ is given by (11), and we adopt the simplest usable form $n^{\text{reg}}(\omega) = a_{\text{coh}}\omega + b_{\text{coh}}$ for the regular part, which is due mainly to $n_0(\omega)$.

Table I gives the results of the calibration fit to the data in Fig. 1, using energies in (30 meV, 50 meV). As Fig. 3 (left panel) shows, the fitting is *good* in this window. This fit gives a quasiparticle broadening $\eta_{\text{coh}} \approx 10 \text{ meV}$ (assumed to be constant over the Brillouin zone and the energy window 30 – 50 meV), uncomfortably large in that $\eta_{\text{coh}}/E_{\text{coh}} \approx 1/4$. We do not know why this exceeds the result $\eta(E_{\text{coh}} \approx 40 \text{ meV}) \approx 1 \text{ meV}$. fitted by Ref. 16 assuming a broadening $\eta(\omega) \propto \omega$.

Now we turn to the fit of the boson feature, using an energy window (80 meV, 140 meV) which contains the hump in Fig. 1, to the fitting form implicit in Eqs. (10) [for $I(\omega)$], (13), and (14):

$$n(\omega) = n_{\text{bos}}^{\text{reg}}(\omega) + \delta n^{\text{sing}}(\omega). \quad (16)$$

Here we take the simplest usable form for the regular part

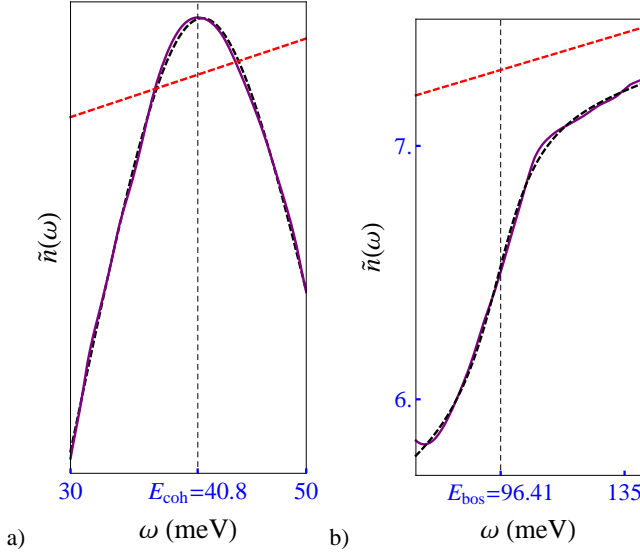


FIG. 3: [COLOR ONLINE] Fit of the experimental DOS $n(\omega)$ to fitting forms, using the windows of energies marked in Fig. 1. (a) Fit of “coherence peak” to Eq. (15), using energies 30–50 meV. (b) Fit of boson feature to Eq. (16), using energies 80–140 meV.

$n_{\text{bos}}^{\text{reg}}(\omega) = a_{\text{bos}}\omega + b_{\text{bos}}$, representing $n_0(\omega)$ plus regular contributions from $\underline{\Sigma}(E)$. Also from (14) we see

$$\delta n^{\text{sing}}(\omega) = \frac{2ig^2a^2m^*}{(2\pi)^4} \times \text{Im} [I(\omega + i\eta_{\text{bos}}) \cdot f(\omega - E_{\text{bos}} + i\eta_{\text{bos}})] \quad (17)$$

The fitted parameters are given in Table I; the fit (Fig. 3) is *fairly good* in its energy window.

We note that, based on the data from which Fig. 1 is drawn, Ref. [1] identified the bosonic mode energy as 52 ± 8 meV, using the inflection point before the hump, so our result of ~ 56 meV (fitting just one *typical* spectrum) is in agreement with them. The quasiparticle damping was $\eta_{\text{bos}} \approx 11$ meV. Thus $\eta/E(\mathbf{k}) \approx \eta/E_{\text{bos}} \approx 0.11 \ll 1$ in the E_{bos} fit window, verifying the criterion for the Bogoliubov quasiparticles to be well-defined.

A dimensionless measure of coupling strength is the ratio of the logarithmic factors $f(z)$ in the boson feature [Eq. (16)] and coherence peak [Eq. (15)]:

$$\lambda_{\text{log}} \equiv \frac{2g^2|I(E_{\text{bos}} + i\eta_{\text{bos}})|}{(2\pi)^2} \approx 0.057, \quad (18)$$

using the numerical value $|I(E_{\text{bos}} + i\eta_{\text{bos}})| = 8.7 \times 10^{-4}$ meV $^{-2}$, validating our weak-coupling assumption.

Momentum-dependent boson coupling and gap renormalization

What if the electron-boson coupling $g(\mathbf{q})$ in (3) is not constant but depends on the electron momentum transfer \mathbf{q} ? Firstly, it gives renormalizations of $\Delta(\mathbf{k})$ due to Σ_{12} which is no longer zero (see Eqs.(4) and (5)). To obtain an upper bound for the gap renormalization, we try the form for \mathbf{q} dependence which leads to the maximal renormalization, namely

$|g(\mathbf{q})|^2 = \tilde{g}^2[\frac{1}{2}(\cos q_x + \cos q_y)]$, where we set \tilde{g} to the fitted g value from Table I. We compute the gap renormalization using the obvious generalization to account for \mathbf{q} dependence of electron-boson coupling in (the off-diagonal components of) Eq. 8. We find that for all energies, the gap renormalization is less than 5 meV, which is small enough compared to Δ_0 to justify our weak-coupling assumption, but not so small to categorically rule out some contribution by the boson to pairing.

For the boson feature, the overall structure of the calculation carries through but the self-energy $\underline{\Sigma}$ becomes momentum dependent. We find the same sort of DOS feature, in which “ g^2 ” is now interpreted as a certain weighted average of $|g(\mathbf{q})|^2$ over the Brillouin zone – a lumped parameter in the spirit of the “ $\alpha^2F(\omega)$ ” combination from the strong-coupling formalism [2]. The singularity in the self energy still come from the saddle point in the dispersion of the d -wave BCS quasiparticles, leading to the same qualitative shape (smoothed step + logarithm) for the boson feature.

Conclusion and Discussion

We have shown how a weak-coupling point of view can be used to analyze the high-energy features in the STM data of BSCCO. The ideal analytic shape of the feature is a linear combination of a (rounded) logarithmic-kink and a (rounded) step edge [cf. Eq. (14)]. Our proposed fitting scheme allowed us to extract (1) the boson’s frequency Ω_0 (2) an average electron-boson coupling g , and an estimate of the damping of the d -wave Bogoliubov quasiparticles. Our estimate $\Omega_0 \approx 56$ meV is in agreement with previous estimates from STM data, which were not fully in agreement with ARPES data. Our simplified simple functional form for the boson feature [Eq. (16)] facilitates the vast number of numerical fits required by the extreme spatial inhomogeneity of STM spectra in BSCCO [11, 12, 16]. However, our theory did *not* address the spatial Fourier spectrum of the boson feature [1, 13, 14], which might distinguish the true functional form of $g(\mathbf{q})$ and thus illuminate the nature of the bosonic mode.

In an s -wave superconductor with a dispersionless boson such as ours, the boson feature would cancel completely in our weak-coupling treatment. This may have motivated suggestions [9, 20] that the observed phonon mode was an artifact localized in a surface barrier. However, we found the d -wave quasiparticle dispersion is non-uniform enough to make $\underline{\Sigma}(\omega)$ nonconstant in ω thus producing an DOS feature. As noted after, Eq. (9) so long as we have a momentum-independent electron-phonon coupling to an Einstein oscillator, no off-diagonal self-energy contribution is generated, and hence the d -wave gap is *not* renormalized.

Our approach was agnostic as to the pairing mechanism. If the fitted g respects the weak-coupling assumption, as we found, it can be inferred that the boson producing the STM feature is *not* contributing to the pairing; if the weak-coupling assumption is violated, we can only conclude that the boson *perhaps* plays a role in the mechanism. To resolve that question, one must see if a proper strong-coupling Eliashberg calculation predicts a pairing amplitude Δ_0 comparable to the observed value.

We thank J. C. Davis, J. W. Alldredge, D. J. Scalapino, A. Balatsky, P. Hirschfeld, J.-X. Zhu, and M. Fischer for conversations. We also thank J. W. Alldredge and J. C. Davis for providing us with unpublished data sets. This work was supported by NSF grant DMR-1005466 and made use of the Cornell Center for Materials Research computing facilities which are supported through the NSF MRSEC program (DMR-1120296).

-
- [1] Jinho Lee *et al*, Nature 442, 546 (2006).
 [2] W. L. McMillan, and I. M. Rowell, in *Superconductivity Vol. 1*, p. 561 (ed. R. D. Parks: Dekker, New York, 1969).
 [3] D. J. Scalapino, in *Superconductivity Vol. 1*, p. 449 (ed. R.D. Parks: Dekker, New York, 1969); J. P. Carbotte, Rev. Mod. Phys. 62, 1027 (1990); and references therein.
 [4] G. M. Eliashberg, Sov. Phys. JETP 11, 696-702 (1960).
 [5] S. Johnston and T. P. Devereaux, Phys. Rev. B 81, 214512 (2010).
 [6] A. N. Pasupathy *et al*, Science 320, 196 (2008).
 [7] A. V. Balatsky and J. X. Zhu, Phys. Rev. B 74, 094517 (2006).
 [8] S. Johnston *et al*, Phys. Rev. B 82, 064513 (2010).
 [9] Jungseek Hwang *et al*, Nature 446, E3-E4 (2007).
 [10] We adopt the six-parameter fit from M. R. Norman *et al*, Phys. Rev. B 52, 615 (1995): hopping amplitudes to successive neighbors of $t_1 = -147.9$ meV, $t_2 = 40.9$ meV, $t_3 = -13.0$ meV, $t_4 = -14.0$ meV and $t_5 = 12.8$ meV, plus a chemical potential $\mu = 130.5$ meV.
 [11] K. McElroy *et al.*, Science 309, 1048 (2005).
 [12] S. H. Pan, *et al*, Nature 413, 282 (2001); T. Cren *et al* Europhys. Lett. 54, 84 (2001); C. Howald, P. Fournier, and A. Kapitulnik, Phys. Rev. B 64, 100504 (2001); K. M. Lang *et al.*, Nature 415, 412 (2002); A. C. Fang *et al.*, Phys. Rev. B 70, 214514 (2004).
 [13] Jian-Xin Zhu *et al*, Phys. Rev. B 73, 014511 (2006).
 [14] “Effects of pairing potential scattering on Fourier-transformed inelastic tunneling spectra of high-T-c cuprate superconductors with bosonic modes” J.-X. Zhu *et al*, Phys. Rev. Lett. 97, 177001 (2006).
 [15] J. W. Alldredge *et al*, unpublished.
 [16] J. W. Alldredge *et al*, Nature Physics 4, 319 - Apr 2008.
 [17] S. Pujari, Ph. D. thesis, Cornell University (2011), “Explorations in STM Phenomenology: ‘Inversion’ techniques for STM data analysis”. Note that Eqs. (4.15)-(4.16) in the thesis are in error; the corrected formulas are Eqs. (10)-(12) and $I(\omega)$ derived from (10). in the present paper.
 [18] R. C. Jaklevic and J. Lambe, Phys. Rev. Lett. 17, 1139-1140 (1966).
 [19] B. C. Stipe, M. A. Rezaei, and W. Ho, Science 280, 1732-1735 (1998).
 [20] S. Pilgram, T. M. Rice, and M. Sigrist, Phys. Rev. Lett. 97, 117003 (2006).
 [21] We consider only the $\omega > 0$ part of the spectrum for the fitting scheme; the same fitting scheme could be applied to the $\omega < 0$ side.